structed position of the North Atlantic Current and the gyre boundary (Fig. 2). This suggests that the glacial subpolar gyre took on polar characteristics when the subpolar-subtropical gyre boundary shifted to a more zonal orientation and the northward excursion of warm subtropical waters into the subpolar region ceased. This allowed a southern migration of water with polar characteristics. The polar front represents the southern limit of this migration, which occurred at the subpolar-subtropical gyre boundary. This interpretation is consistent with that of Ruddiman and McIntyre (*3*).

We speculate on why the North Atlantic had a more zonally oriented w_e = curl(τ) = 0 line 18,000 years ago. In the present-day North Atlantic, the position of the line where w_e = curl(τ) = 0 corresponds to the location of strong eastward wind stresses (produced by westerlies) and occurs where the meridional gradient of these stresses vanishes (*19*). These strong stresses are due to continental storms. In turn, the southwest to northeast trend of the line is due to the storm tracks, which have a similar pattern. However, in our runs, strong eastward stresses occur only in the eastern central North Atlantic, centered on approximately 35°W, 45°N, as if the present-day pattern had swung to the south. This suggests that the storm tracks 18,000 years ago ran more zonally and farther to the south than they do now, which is consistent with interpretations based on geological data (*20*).

Central to our hypothesis is that the buildup of a substantial ice cap is necessary before the paleowind fields can be expected to shift and, in turn, alter the orientation of the gyre boundary. Changes in ice volume should precede changes in SST. Using oxygen isotope analyses and assemblages of planktonic foraminifera from the same core, Ruddiman and McIntyre (*3*) have shown that continental glaciation preceded changes in SST as far north as 60°N in the North Atlantic during the isotopic 5 to 4 and 5e to 5d transitions approximately 120,000 years ago. This sequence of events implies that the ocean passively responds to continental ice conditions rather than actively driving an ice age and the consequential buildup of continental ice. Our interpretation accounts only for changes in the ocean over the relatively long time scales of continental ice buildup and decay. It does not explain the much more rapid (approximately 1000-year) Younger Dryas event, which did not correspond with any substantial change in ice coverage (*21*).

Our scenario for the role of the ocean during glaciation can be summarized as follows. Low summer insolation causes accumulation of snow and ice through the summer, which in turn increases the volume of ice and overall earth albedo. The ice volume eventually becomes large enough to influence thermal and orographic steering of the w_e = curl(τ) = 0 line, causing it and, by consequence, the subtropical-subpolar gyre boundary to move southward. Finally, such a shift shuts off the supply of warm and salty waters to the high-latitude North Atlantic, resulting in a drop in SST and a cessation of bottom water production in the high latitudes. Deglaciation follows a similar, but reversed, sequence (*22*).

REFERENCES AND NOTES

1. A. V. Bunker and L. V. Worthington, *Bull. Am. Meteorol. Soc.* **57**, 670 (1976).
2. CLIMAP, *Geol. Soc. Am. Map Ser. MC-36* (1981).
3. W. F. Ruddiman and A. McIntyre, *J. Geophys. Res.* **82**, 3877 (1977).
4. B. A. Warren, *J. Mar. Res.* **41**, 327 (1983).
5. For a review, see B. H. Corliss, D. G. Martinson, T. Keffer, *Geol. Soc. Am. Bull.* **97**, 1106 (1985).
6. W. F. Ruddiman, in *North America and Adjacent Oceans During the Last Deglaciation*, W. F. Ruddiman and H. E. Wright, Jr., Eds. (Geological Society of America, Boulder, CO, in press).
7. T. Keffer, B. H. Corliss, D. G. Martinson, *Eos* **67**, 44 (1986).
8. R. E. Newell and J. Hsiung, in *Abrupt Climatic Change*, W. H. Berger and L. D. Labeyrie, Eds. (Reidel, Dordrecht, 1987), pp. 67–87.
9. W. H. Munk, *J. Meteorol.* **7**, 79 (1950).
10. H. Stommel, *The Gulf Stream* (Univ. of California Press, Berkeley, 1965).
11. The CLIMAP (*2*) geological indices have been used to calculate present-day SSTs (*12*). In the region of interest, these geologically based SSTs are nearly indistinguishable from the observed SSTs, except for an area southeast of Newfoundland where the geologically based estimates are warmer than observed by ≥1.2°C.
12. B. Molfino *et al.*, *Quat. Res. (N.Y.)* **17**, 279 (1982).
13. A. Leetma and A. F. Bunker, *J. Mar. Res.* **36**, 311 (1978).
14. H. U. Sverdrup, M. W. Johnson, R. H. Fleming, *The Oceans* (Prentice-Hall, New York, 1942).
15. I. M. Held, *Icarus* **50**, 449 (1982).
16. S. Manabe and A. J. Broccoli, *J. Geophys. Res.* **90**, 2167 (1985).
17. For examples of other atmospheric simulations for 18,000 years before present, see J. Williams *et al.* [*J. App. Meterol.* **13**, 305 (1974)], W. L. Gates [*Science* **191**, 1138 (1976)], and J. E. Kutzbach and P. J. Guetter [*J. Atmos. Sci.* **43**, 1726 (1986)].
18. E. J. Barron and W. M. Washington, *J. Geophys. Res.* **89**, 1267 (1984).
19. This is because of the dominance of zonal winds and the near similarity of Ekman pumping and wind stress curl. This allows Ekman pumping to be approximated as $w_e \sim \text{curl}(\tau) \sim \partial\tau(x)/\partial y$. Hence, where the meridional gradient of zonal wind stress $[\partial\tau(x)/\partial y]$ equals zero, w_e will tend to equal zero.
20. W. F. Ruddiman and A. McIntyre, *Science* **204**, 173 (1979).
21. W. S. Broecker, D. M. Peteet, D. Rind, *Nature* **315**, 21 (1985).

22. We thank E. Barron and L. Sloan (both at Pennsylvania State University) for providing wind stress values for 18,000 years before present. This research was initially supported by a grant from the Woods Hole Oceanographic Institution Center for the Analysis of Marine Systems. Additional support came from NSF grants OCE 83-15369 and OCE 85-15642 (T.K.), and OCE-84-19595 and OCE-86-14162 (B.H.C.). This is University of Washington, School of Oceanography contribution number 1776 and Lamont-Doherty Geological Observatory number 4299.

22 February 1988; accepted 2 June 1988

Direct Measurement of O_2-Depleted Microzones in Marine *Oscillatoria*: Relation to N_2 Fixation

HANS W. PAERL AND BRAD M. BEBOUT

Among the nitrogen (N_2)-fixing cyanobacteria, the filamentous, nonheterocystous marine *Oscillatoria* spp. (*Trichodesmium*) appears enigmatic; it exhibits N_2 fixation in the presence of oxygenic photosynthesis without structural protection of the N_2-fixing apparatus (nitrogenase) from potential inhibition by molecular oxygen (O_2). Characteristically, N_2 fixation is largely confined to aggregates (bundles) of filaments. Previous work has suggested that spatial partitioning of photosynthesis and of N_2 fixation occurs in the bundles as a means of allowing both processes to occur contemporaneously. The probing of freshly sampled bundles with O_2 microelectrodes directly confirmed such partitioning by showing the presence of O_2-depleted (reduced) microzones in photosynthetically active, N_2-fixing bundles. Bundle size was directly related to both the development of internal reduced microzones and cellular N_2 fixation rates. By enhancing microzone formation, bundles optimize N_2 fixation as a means of supporting *Oscillatoria* spp. blooms in surficial, nitrogen-depleted tropical and subtropical waters.

TROPICAL AND SUBTROPICAL NITROGEN-depleted marine waters periodically support near-surface blooms of the filamentous oxygenic cyanobacterium *Oscillatoria* (*Trichodesmium*) spp. Blooms are confined to calm periods when buoyant filaments accumulate at the surface as red-dish-brown aggregates or bundles. The filaments in the bundles are oriented in a parallel fashion (Fig. 1). Characteristically, N_2 fixation is associated with bundles (*1*).

Institute of Marine Sciences, University of North Carolina, Chapel Hill, Morehead City, NC 28557.

Previous studies concur that *Oscillatoria* spp. blooms are responsible for relatively high rates of planktonic N_2 fixation, which constitute ecologically significant inputs of combined nitrogen (*2*).

The mechanisms that allow *Oscillatoria* spp. to fix N_2 in the presence of oxygenic photosynthesis have not been directly identified. The N_2-fixing enzyme complex, nitrogenase, is readily inactivated by molecular O_2 in a variety of cyanobacteria and eubacteria (*3*). Whereas some filamentous N_2-fixing cyanobacteria form biochemically and structurally distinct O_2-devoid cells termed heterocysts in which nitrogenase is localized (*4*), *Oscillatoria* spp. reveal no cellular differentiation. This organism is exceedingly difficult to culture, which has hindered our understanding of how contemporaneous photosynthetic O_2 evolution and N_2 fixation can take place.

Field observations reveal that N_2-fixing capabilities of *Oscillatoria* spp. are closely linked to the extent of bundle formation (*1, 5*). Whereas large bundles composed of from tens to several hundred filaments exhibit light-mediated N_2 fixation, individual filaments or small aggregates (two to ten filaments) often fail to fix N_2 (*1*). Accordingly, on calm days when filaments readily aggregate as bundles in surface slicks, N_2 fixation rates per unit biomass are maximal, whereas wind-induced turbulence leads to decreases in both average bundle size and biomass-specific N_2 fixation (*1, 5*). Using autoradiography, Carpenter and Price showed (*1*) that $^{14}CO_2$ fixation was unevenly distributed along filaments; $^{14}CO_2$ fixation was confined to terminal portions of the filaments whereas intercalary regions exhibited extremely low rates of fixation. On the basis of these observations, they suggested that N_2 fixation could accompany photosynthesis if the processes remained spatially separated within filaments. When filaments were aggregated as bundles, a three-dimensional O_2-depleted internal portion, composed of parallel intercalary regions, might be a likely site of N_2 fixation.

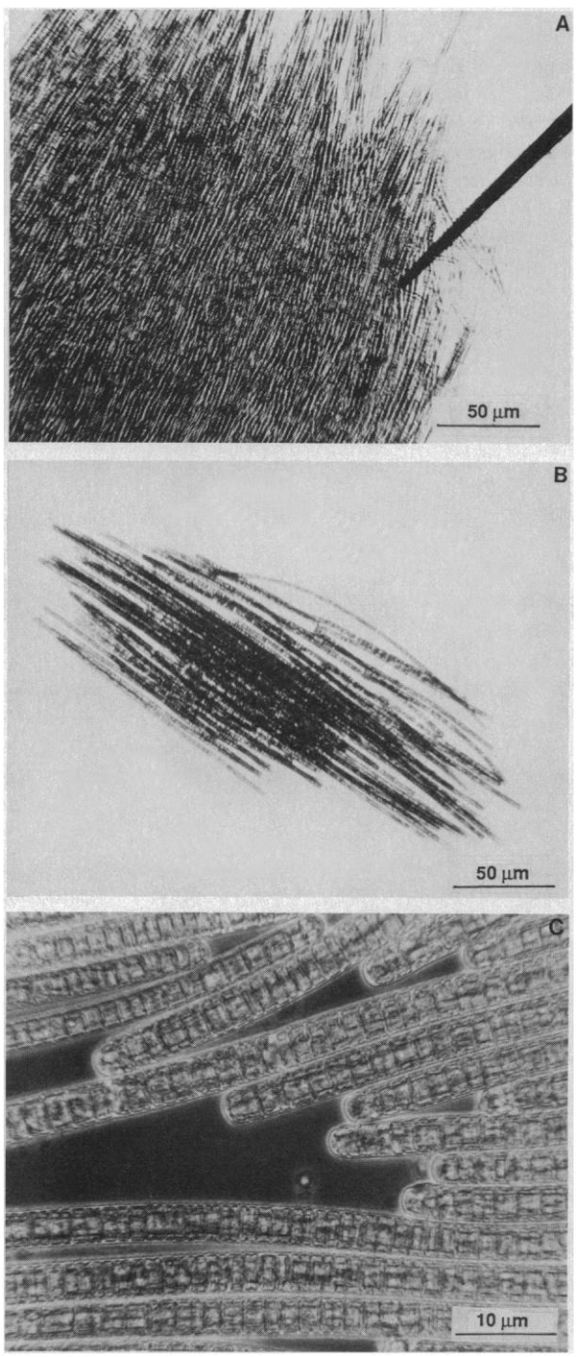

Fig. 1. (**A**) A segment of a large (>75 filaments) *Oscillatoria* spp. bundle that has a parallel arrangement of individual filaments. The tip of an O_2 microelectrode (tip diameter approximately 7 μm) is shown inserted into the bundle. Bundles of this size frequently revealed internal O_2-depleted microzones. (**B**) A relatively small bundle consisting of approximately 30 individual filaments. Internal reduced microzones were not evident in such bundles. (**C**) High-magnification view of individual filaments arranged in bundles. Bright, granular intracellular structures are gas vacuoles, which greatly enhance buoyancy, thus promoting surface accumulations of bundles during calm conditions.

By using O_2 microelectrodes in combination with N_2 fixation (acetylene reduction) measurements, we have directly confirmed the presence of internal O_2-depleted (reduced) microzones in photosynthetically active, N_2-fixing *Oscillatoria* spp. bundles. Both the extent of bundle size and its configuration are determinants in reduced microzone formation and resultant N_2 fixation capacity.

Unusually calm, warm, and clear weather, combined with the close proximity of subtropical Gulf Stream waters to North Carolina's coastline (*6*), led to several *Oscillatoria* spp. blooms during October and November 1987. These climatic conditions also favored the parallel development of toxic dinoflagellate (*Ptychodiscus breve*) blooms (red tides) (*7*). *Oscillatoria* spp. blooms were often spatially separated from *Ptychodiscus* blooms, hence facilitating exclusive sampling and analysis of the *Oscillatoria* (*8, 9*).

We measured O_2 concentrations surrounding and within individual *Oscillatoria* spp. bundles, using microelectrodes (*10*). These microelectrodes had sensing tips 3 to 7 μm wide and a spatial resolution of 100 μm. Bundles were placed in small plastic petri dishes containing seawater and a glass fiber filter. The bundles were held immobile with a few teased-up fibers on the filter. Microelectrode O_2 profiles in ambient seawater and bundles were initiated within 1 to 2 min after the placement of bundles in petri dishes. Electrode tips were positioned by a micromanipulator while the specimen was observed under a dissecting microscope. Electrode polarization voltage was supplied by, and current output recorded with, a chemical microsensor (Diamond Electrotech model 1201). The electrode output was calibrated against air-bubbled seawater (100% of saturation of O_2) and N_2-bubbled seawater (0% of saturation of O_2). All oxygen measurements were made within 5

hours of sample collection under illuminated (200 to 1140 μE m^{-2} S^{-1}) and dark conditions. To test for the production of abiotic oxygen gradients, we heat-killed some bundles by placing them in a microwave oven for ≈5 s, which raised the temperature of the small volume of seawater in the petri dish sufficiently to kill *Oscillatoria* spp. cells without destroying the structure of the bundles.

Distinct differences in the rates of chlorophyll a–normalized nitrogenase activity (NA) were observed among bundles of various sizes, with large bundles generally exhibiting much greater rates than small bundles (Table 1). Reduction of bundle size, induced either by teasing bundles apart (by using a 25-gauge syringe needle) or by vigorous shaking, led to a marked reduction in NA. In all cases NA was strongly light dependent.

Microelectrode measurements revealed regions of O_2 concentration markedly lower than ambient both within and surrounding *Oscillatoria* spp. bundles (Fig. 2). The lowest O_2 concentrations were within the central portions of the bundles, whereas O_2 concentrations in terminal regions of the bundles were only slightly lower than ambient. Highly dynamic photosynthetic processes appeared to be responsible for the distribution of O_2 near bundles. We recorded O_2 concentrations in excess of 200% of saturation in terminal regions immediately (within 2 min) after increases in light intensity from 200 to 1140 μE m^{-2} S^{-1} of photosynthetically active radiation (PAR). Completely shading a bundle (1140 to 0 μE m^{-2} S^{-1} PAR) reduced the O_2 concentration from 200% of saturation to 75% of saturation within 1 min. "Steady-state" O_2 concentrations (1140 μE m^{-2} S^{-1}) were generally 75 to 100% of saturation. Under "steady-state" conditions, the bundles were able to rapidly deplete O_2 in the water immediately surrounding them, resulting in measurable boundary layers as far as 500 μm from the bundle surfaces. Microelectrode profiles of heat-killed bundles revealed neither O_2-depleted microzones nor boundary layers (Fig. 3). The O_2 concentrations in the heat-killed samples were slightly lower than in live samples as a result of the lower solubility of O_2 in the previously heated seawater.

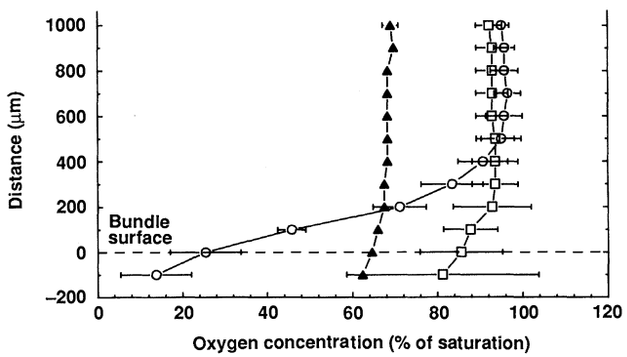

Fig. 2. Vertical distribution of dissolved O_2 concentrations near the ends (□) and middle (○) segments of large *Oscillatoria* spp. bundles, as determined with O_2 microelectrodes. Each value indicates the mean and standard error of three replicate bundles. Lower O_2 concentrations in the heat-killed bundles (▲) are likely due to both a cessation of photosynthesis and the reduced solubility of O_2 in the previously heated seawater.

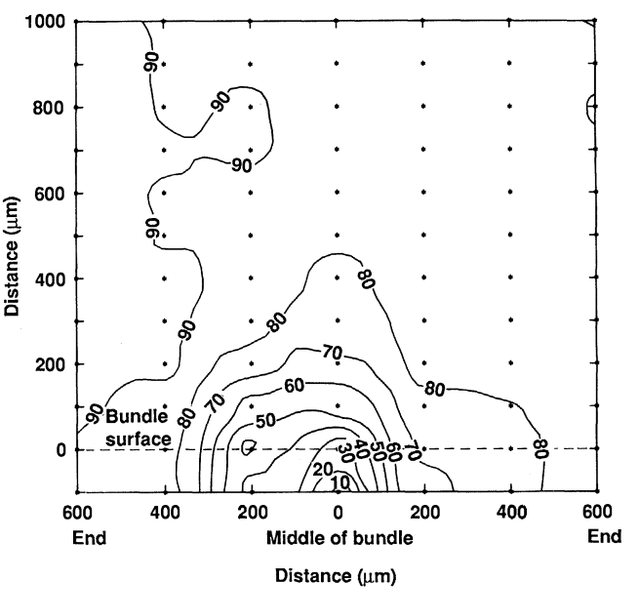

Fig. 3. Distribution of dissolved O_2 concentrations near and within an *Oscillatoria* spp. bundle. Points at which O_2 microelectrode determinations were made are indicated (asterisks).

Bundles incubated for 48 hours in 500-ml Erlenmeyer flasks (200 μE m^{-2} S^{-1} PAR; 12 hours light:12 hours dark) revealed decreases in both NA and internal O_2-depleted microzone formation. This response was observed among bundles of various sizes. These decreases were not a result of loss of viability, because the photosynthetic O_2 production characteristics of bundles remained high. Decreases in NA may have resulted from nitrogen regeneration by associated bacteria and protozoans, which may have replaced N_2 fixation as the chief means of meeting nitrogen demands among *Oscillatoria* spp. bundles under confined conditions. In any event, a loss of NA paralleled the disappearance of O_2-depleted microzones among such bundles.

In concert, these results directly confirm Carpenter and Price's contention that N_2 fixation and oxygenic photosynthesis are compatible in bundles of morphologically undifferentiated *Oscillatoria* spp. filaments (*1*). Bundle size and tightness are directly related to the extent of reduced microzone formation and NA. As such, climatic conditions, specifically water column turbulence combined with adequate irradiance, which dictate bundle size and photosynthetically generated energy availability, are determinants that mediate marine N_2 fixation inputs attributable to *Oscillatoria* spp. Although wind-induced turbulence can negate NA of *Oscillatoria* spp. by breaking up bundles, resultant vertical mixing of individual filaments and small aggregates leads to enhanced exposure to ambient inorganic and

Table 1. Comparative acetylene reduction (AR) rates for freshly collected small versus large bundles of *Oscillatoria* spp. Each replicate represents a sample containing at least 20 small or 10 large bundles. Care was taken to select bundles similar in shape and size for each treatment. The background rate of ethylene production (ethylene contamination in acetylene plus ethylene production in 0.4 μm of filtered seawater) was 1.5 nmol/liter per hour; this rate was subtracted from *Oscillatoria* AR rates; chlorophyll a, Chl a.

Bundle	Chl a (μg/liter)	AR (nmol/liter per hour)	AR: Chl a (nanomoles per microgram of Chl a per hour)
Small bundles (<30 filaments per bundle)			
1	120	29.5	0.246
2	125	30.5	0.244
3	110	30.0	0.273
			Average = 0.254, SEM = 0.016
Large bundles (>75 filaments per bundle)			
1	110	220.5	2.00
2	105	240.5	2.29
3	115	235.0	2.04
			Average = 2.11, SEM = 0.157

organic combined nitrogen. Among vertically mixed individual filaments, cellular surface to volume ratios are increased while transport to deeper, combined nitrogen–enriched waters is enhanced. In this manner, N_2 fixation is optimized as a means of obtaining combined nitrogen on calm days, whereas ambient combined nitrogen usage becomes more feasible under turbulent conditions.

Although we have shown the existence and roles of O_2-depleted microzones, the means by which intercellular "division of labor" among oxygenic photosynthesis and O_2-sensitive N_2 fixation is induced and maintained are currently unresolved. Transport of photosynthetically produced carbon compounds to O_2-depleted N_2-fixing cells must take place to provide both reductant and carbon skeletons essential as an energy source for N_2 fixation and for accepting (incorporating) recently fixed NH_3. Although transport of photosynthetically fixed $^{14}CO_2$ to internal O_2-depleted microzones can be shown by autoradiography, the genetic, physiological, and structural mechanisms that mediate such transport remain unknown.

REFERENCES AND NOTES

1. E. J. Carpenter and C. C. Price IV, *Science* **191**, 1278 (1976).
2. E. J. Carpenter and D. G. Capone, Eds., *Nitrogen in the Marine Environment* (Academic Press, New York, 1983), p. 521.
3. F. R. S. Postgate, *The Fundamentals of Nitrogen Fixation* (Cambridge Univ. Press, Cambridge, 1982).
4. C. P. Wolk, in *The Biology of Cyanobacteria*, N. G. Carr and B. A. Whitton, Eds. (Blackwell, Oxford, 1982), p. 359.
5. I. Bryceson and P. Fay, *Mar. Biol.* **61**, 159 (1981).
6. The location of the Gulf Stream with respect to North Carolina's coastline is routinely determined by satellite imagery and by field measurements conducted by the National Oceanographic and Atmospheric Administration–National Marine Fisheries Service Laboratory, Beaufort, NC. During October–November 1987, water masses representing the western wall of the Gulf Stream were as close as 2 km to Cape Lookout and Beaufort Inlet, NC.
7. P. Tester and R. Ferguson, personal communication.
8. Near-surface water samples were taken with precleaned 2-liter wide-mouth polypropylene jars at several Atlantic coastal locations 1.6 to 4.8 km seaward from Beaufort Inlet. Jars were transported (within 2 hours) at surface water temperature to the laboratory. We immediately examined buoyant *Oscillatoria* spp. bundles, of various sizes and shapes, for N_2-fixing and photosynthetic O_2 production capabilities by using acetylene reduction assays (*9*) and O_2 microelectrode measurements (*10*). Bundles were removed from jars with a large-bore polypropylene pipette. For acetylene reduction assays, 20-ml samples, containing either large (>75 filaments) or small (<30 filaments) bundles, were dispensed into 25-ml borosilicate Erlenmeyer flasks. Three replicate flasks were used for each size class. Flasks were sealed with rubber serum stoppers, inverted, and injected with 2 ml of ultrahigh-purity acetylene (Matheson). Flasks were incubated on their sides under nonshaken conditions for 2 to 4 hours at surface water temperatures. Chlorophyll a–specific NA was determined under both illuminated (200 $\mu E\ m^{-2}\ S^{-1}$ PAR; combined cool white and Sylvania Grow-Lux fluorescence) and dark conditions. After incubation, all flasks were shaken to equilibrate aqueous and gas phases and a 0.3-ml headspace gas sample was withdrawn and injected into a Shimadzu GC-9A flame ionization gas chromatograph having a 2-m-long Poropak T column held at 80°C. Ethylene production was calibrated against ultrahigh-purity ethylene (Matheson) standards.
9. W. D. P. Stewart, C. R. Fitzgerald, R. H. Burris, *Proc. Natl. Acad. Sci. U.S.A.* **58**, 2071 (1967); H. W. Paerl and P. E. Kellar, *J. Phycol.* **14**, 254 (1978).
10. N. P. Revsbech, in *Polarographic Oxygen Sensors*, E. Graiger and H. Forstner, Eds. (Springer-Verlag, Berlin, 1983), p. 265; R. G. Carlton and R. G. Wetzel, *Can. J. Bot.* **65**, 1031 (1987).

11. Supported by NSF grants OCE 85-00740 and BSR 86-14951 and by the North Carolina Biotechnology Center (Project 86-G-01013). We thank R. G. Carlton, L. E. Prufert, J. Garner, H. Page, and V. Page for technical assistance.

28 January 1988; accepted 20 May 1988

Translation in Mammalian Cells of a Gene Linked to the Poliovirus 5′ Noncoding Region

DIDIER TRONO,* JERRY PELLETIER, NAHUM SONENBERG, DAVID BALTIMORE

The central portion (region P) of the 742-nucleotide noncoding 5′ end of poliovirus allows the RNA to initiate protein synthesis in the absence of the usual 5′ 7-methylguanosine capping group. Poliovirus 5′ noncoding region was fused to a reporter gene and transfected into cells. There was extensive augmentation of the expression of this gene by poliovirus-mediated inhibition of cap-dependent protein synthesis. That the construct initiated in a cap-independent manner was verified through in vitro experiments. Small lesions throughout region P blocked its initiation function, implying that a coherent functional unit, hundreds of nucleotides long, is responsible for cap-independent initiation by poliovirus RNA.

THE GENOME OF POLIOVIRUS IS A single-stranded molecule of plus-strand RNA, approximately 7500 bases long (*1*). Poliovirus has an unusually long 5′ noncoding region, which consists of 742 untranslated nucleotides preceding the AUG used to initiate translation (*2*). A highly significant sequence similarity extends through the first 650 nucleotides of the three poliovirus serotypes (*3*), an indication that the region has a crucial role in the viral life cycle. Poliovirus messenger RNA, unlike most other eukaryotic mRNAs, is not capped at its 5′ end; it terminates in pUp instead of the usual "capping group" $m^7G(5')ppp(5')N...$ (*4*). It must therefore be translated in a cap-independent manner. The virus takes advantage of its unique style of translation initiation to inhibit cellular protein synthesis by interfering with the cap-dependent translation of cellular mRNAs (*5*).

Using a cDNA copy of the viral genome (type 1, Mahoney) (*6*), we engineered a number of mutations into the poliovirus 5′ noncoding region (*7*). The biochemical and genetic analysis of several phenotypically recognizable viral strains thereby generated showed that an RNA sequence of hundreds of nucleotides (which we called region P) is involved in allowing viral protein synthesis (*7*). In vitro experiments also suggested that a large portion of the poliovirus 5′ noncoding region is responsible for the cap-independent translation of downstream sequences (*8*). So far, no cellular gene has been

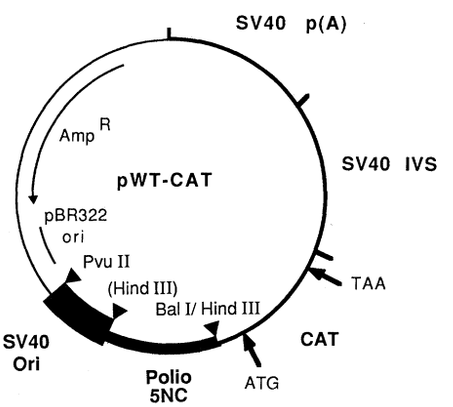

Fig. 1. Schematic representation of the wild-type construct (pWT-CAT). Nucleotides 1 to 630 of poliovirus type 1 (Mahoney) (*1*) were cloned in the Hind III site of the pSV2CAT plasmid (*9*); in the other constructs, the corresponding region of various mutated clones (*7*) was substituted for the wild-type sequence.

D. Trono, Whitehead Institute for Biomedical Research, Cambridge, MA 02142.
J. Pelletier and N. Sonenberg, Department of Biochemistry, McGill University, Montreal, Quebec, Canada H3G 1Y6.
D. Baltimore, Whitehead Institute of Biomedical Research, Cambridge, MA 02141, and Department of Biology, Massachusetts Institute of Technology, Cambridge, MA 02139.

*To whom correspondence should be addressed.